An Analog CMOS Central Pattern Generator for Interlimb Coordination in Quadruped Locomotion

Kazuki Nakada, *Student Member, IEEE*, Tetsuya Asai, *Member, IEEE*, and Yoshihito Amemiya, *Member, IEEE*

Abstract—This paper proposes a neuromorphic analog CMOS controller for interlimb coordination in quadruped locomotion. Animal locomotion, such as walking, running, swimming, and flying, is based on periodic rhythmic movements. These rhythmic movements are driven by the biological neural network, called the central pattern generator (CPG). In recent years, many researchers have applied CPG to locomotion controllers in robotics. However, most of these have been developed with digital processors and, thus, have several problems, such as high power consumption. In order to overcome such problems, a CPG controller with analog CMOS circuit is proposed. Since the CMOS transistors in the circuit operate in their subthreshold region and under low supply voltage, the controller can reduce power consumption. Moreover, low-cost production and miniaturization of controllers are expected. We have shown through computer simulation, such circuit has the capability to generate several periodic rhythmic patterns and transitions between their patterns promptly.

Index Terms—Analog CMOS circuits, central pattern generator (CPG), coupled neural oscillators, interlimb coordination, quadruped locomotion.

I. INTRODUCTION

ANIMAL locomotion, such as walking, running, swimming and flying, is based on periodic rhythmic movements. These rhythmic movements are driven by the biological neural network, called the central pattern generator (CPG) [1]. CPG consists of sets of neural oscillators, situated in ganglion or spinal cord. Induced by inputs from command neurons, a CPG generates a rhythmic pattern of nerve activity unconsciously and automatically. Such a rhythmic pattern activates motor neurons, thus the rhythmic movements of animals are driven. While not necessary for rhythmic movements, sensory feedback regulates the frequency and phase of these rhythmic patterns generated by CPG [2]. Furthermore, CPG can also adapt to various environments to change the periodic rhythmic pattern itself [3]. For instance, vertebrates, such as horses and cats, can change their locomotor patterns depending on the situation [4], [5]. Since the degree of the freedom of physical parts relevant to locomotion is very high, the coordination of the physical parts, such as interlimb coordination, is required for smooth locomotion. The rhythmic movements driven by CPG induce this coordination. Therefore, CPG plays significant roles in locomotion.

In recent years, many researchers have applied such functions of CPG to locomotion control in robotics [7]–[13]. For example, quadruped robots capable of adapting to irregular terrain using CPG dynamics have been developed by Kimura *et al.* [7]. Billard and Ijspeert have applied a CPG controller to an entertainment robot, AIBO [8]. Shan and Nagashima have proposed a CPG controller for a humanoid robot [9].

In robotics, using CPG for locomotion control has the following advantages: 1) The amount of calculation required for movement control is reduced as a result of the coordination of physical parts induced by the rhythmic movements and 2) As a result of synaptic plasticity which change the configuration of CPG and the rhythmic pattern, high autonomous adaptation to various environments is achieved [10].

In the present paper, we propose an analog CPG controller for the coordination of physical parts in quadruped walking robots. Although a number of CPG controllers have been developed, most of these have been implemented by using digital processors [7]–[9]. While a digital processor can operate with high accuracy, it consumes high power and occupies a large area of chip. Such problems occur to degrade CPG controllers. In order to overcome such problems, the proposed CPG controller is designed as an analog CMOS circuit. As a result, it can reduce power consumption. Moreover, low-cost production and miniaturization of controllers are expected.

CPG controllers as an analog circuit have already been implemented in previous works [11]–[13]. For example, an analog CPG controller for a quadruped walking machine has been proposed by Still and Tilden [11]. Patel *et al.* designed an analog CPG chip based on the Morris–Lecar neurons for intersegmental coordination of an artificial lamprey [12]. Lewis *et al.* proposed a custom analog very large-scale integration (VLSI) chip as a CPG controller, which makes use of the integrated and fire neurons [13].

The present work differs from these works in several respects. First, our CPG controller is based on the Amari–Hopfield neurons [14], which is suitable for analog circuit implementation. Second, it is capable of producing various rhythmic patterns and changing these patterns promptly.

The present paper is organized as follows. In Section II, the biological background of the present work is stated. In Section III, we describe a CPG network model for controlling interlimb coordination in quadruped locomotion. In Section IV, we proposed the circuit architecture of the CPG controller. In Section V, by using computer simulator SPICE, we confirm that

the proposed controller has the capability to produce various rhythmic patterns and transitions from one pattern to another. The further considerations are shown in Section VI. The summary over the present research is presented in Section VII.

II. NEURAL CONTROL OF RHYTHMIC MOVEMENTS

In this section, we describe the fundamental roles of the neural control of rhythmic movements of CPG.

A. Central Pattern Generator

The rhythmic movements of animals, such as locomotion and breathing, are driven by CPG. CPG generates a periodic rhythmic pattern of nerve activity that activates motor neurons, resulting in rhythmic movements of animals. The periodic rhythmic pattern of nerve activity can be regarded as an attractor like a limit cycle, embedded in network structure of CPG. Characteristics of the rhythmic pattern as an attractor contribute to the stability of rhythmic movements. While not necessarily for generating a periodic rhythmic pattern, sensory feedback regulates the frequency and phase of the rhythmic pattern. Sensory feedback balances effects of unexpected and unwanted disturbances by regulating the rhythmic pattern of nerve activity, and thus rhythmic movements driven by CPG are stabilized further.

B. Coordination of Physical Parts

In vertebrate locomotion, one of the most fundamental roles of CPG is to control of each limb. As a result of interaction with CPGs that actuate muscles at each joint of the limbs, rhythmic movements of each of the limbs are stabilized. Another one is cooperation between the limbs, i.e., interlimb coordination. CPGs that control each of the limbs are synchronized via coordinating interneuros between the CPGs, and thus the interlimb coordination is achieved. Since the degree of the freedom of physical parts relevant to locomotion is very high, the coordination of physical parts is required for smooth locomotion. Therefore, CPG can be said to play the central role in locomotion.

C. Rhythmic Pattern Transitions

In rhythmic movements of animals, a transition of the rhythmic movements is often observed. As a typical example, the horse has chosen a locomotor pattern, which is called the gait [4]. It is believed that the optimal gait pattern is chosen based on locomotor speed or the rate of energy consumption [5]. In addition, each gait pattern, such as walk, trot, and gallop, is characterized by the relative phase between the limbs. Fig. 1(a) and (b) shows the typical gait patterns of mammals and its relative phases. Here, LF, LH, RF, and RH represent left forelimb, left hindlimb, right forelimb, and right hindlimb, respectively. The gait patterns are also regarded as different modes of coordination of the limbs. Furthermore, it is considered that gait pattern transitions arise from changing of cooperation of CPGs that control the interlimb coordination.
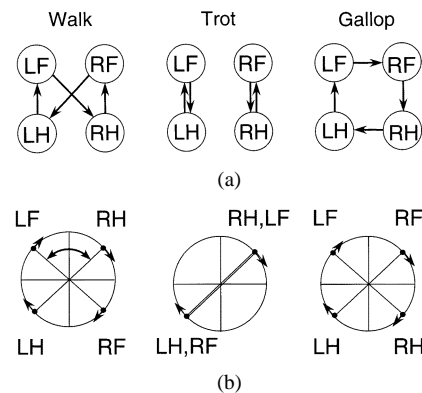

Fig. 1. (a) Typical gait patterns in quadruped locomotion. (b) Relative phases between the limbs in the different gait patterns.
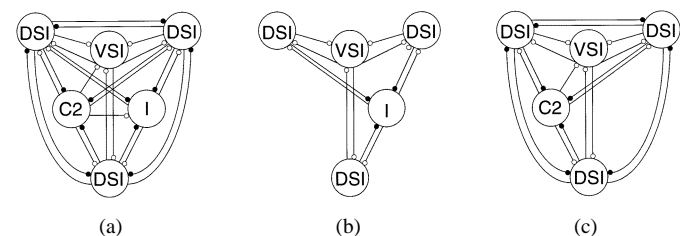

Fig. 2. Examples of *functional reconfigurations* of CPG. (a) Entire network of *Tritonia* swimming CPG. (b) Functional configuration—defensive withdraw mode. (c) Swimming mode. Here, black and white circles represent excitatory and inhibitory synapses, respectively.

D. Functional Reconfiguration of CPGs

Recently, it has been found that neuromodulators, such as serotonin, cause *functional reconfigurations* that produce different rhythmic patterns in individual CPGs [6].

In the *Tritonia* swimming CPG network, two functional configurations, one of them produces defensive withdrawal, the other swimming, could exist [Fig. 2(a)–(c)]. Here, DSI and VSI represent the dorsal swim interneuron and the ventral interneuron, respectively. I is the inhibitory neuron, which mediates DSI to DSI inhibition, and C2 is the cerebral cell 2, which inhibits I neuron. When serotonin induces C2 neuron to release more transmitters and strengthens its synaptic interaction, *functional reconfiguration* is induced [6].

It is considered that such *functional reconfiguration* could exist in CPG networks that control coordination of physical parts of higher vertebrates.

III. CPG MODEL

In this section, we describe a CPG model underlying an analog CPG controller for interlimb coordination in quadruped locomotion.

A. Neural Oscillator Model

A number of artificial neural networks have been proposed as the CPG model [16]–[22]. In the earliest research, Brown proposed the most fundamental CPG model using the neural oscillator, which consists of two neurons and has interactions between neurons by reciprocal inhibition [16]. The model is also one of the relaxation oscillators. Although its configuration is very simple, it is essential as the component of the CPG model.
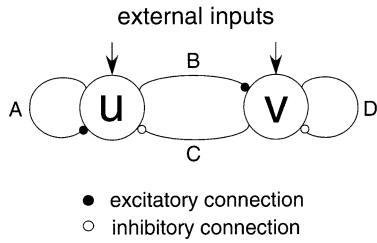
Fig. 3.   Amari–Hopfield neurons model.

In this paper, we chose the Amari-Hopfield neurons model [14] as the neural oscillator. The model consists of an excitatory neuron and an inhibitory neuron with excitatory inhibitory connections (Fig. 3). The dynamics of the Amari-Hopfield model is expressed by the following equations:

$$\begin{cases} \tau\dot{u} = -u + A{\cdot}f_\mu(u) - C{\cdot}f_\mu(v) + S_u(t) \\ \tau\dot{v} = -v + B{\cdot}f_\mu(u) - D{\cdot}f_\mu(v) + S_v(t) \end{cases} \quad (1)$$

where u and v express the activities of the excitatory neurons and the inhibitory neurons, respectively. The parameters A–D determine the dynamics of the model. $S_u(t)$ and $S_v(t)$ express the external inputs. The transfer function $f(x)$ is given by the following equation:

$$f_\mu(x) = \frac{1 + \tanh(\mu x)}{2} \quad (2)$$

where $\tanh(x)$ is the hyperbolic tangent function and μ is its control parameter. The Amari–Hopfield model is suitable for implementation of the CPG model as analog circuits because of its simple transfer function. Its details are given in Section IV-A. Furthermore, the Amari–Hopfield model corresponds to the affine transformation of the Wilson–Cowan neurons model, which imitates the population activities of cortical neurons [15]. Therefore, the qualitative property of both models is equivalent. The dynamics of both models have been studied in detail. Depending on the parameters A through D and the external inputs $S_u(t)$ and $S_v(t)$, the Amari–Hopfield model generates the periodic pattern automatically. Fig. 3 show an attractor of the Amari-Hopfiled model in the $u - v$ phase plane.

B. Neural-Network Model

We composed a neural network model underlying the CPG controller to perform interlimb coordination in quadruped locomotion. As the CPG controller for interlimb coordination, it is desirable to generate various rhythmic patterns. Hence, we constructed a neural-network model from the Amari–Hopfield model according to the neural network proposed by Nagashino *et al.* [19]. Their model consists of four coupled neural oscillators with excitatory and inhibitory interneurons. By introducing the interneurons and switching their interactions with neural oscillators, *functional reconfigurations* of the CPG network are performed, and then various rhythmic patterns are generated [19].

Fig. 5 shows the basic structure of the neural–network model. Here, we describe configurations of networks that generate periodic rhythmic patterns corresponding to each of the typical gaits of mammals. Fig. 6(a)–(c) correspond to the walk mode, the trot mode, and the gallop mode, respectively [19].
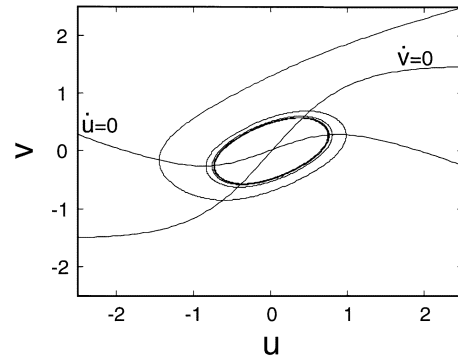

Fig. 4.   Attractor of the Amari–Hopfield model in the $u - v$ phase plane. The limit-cycle: $A = C = 4.0$, $B = 3.0$, $D = 0.0$, $S_u = 0.0$, $S_v = -1.5$, and $\mu = 1.0$.
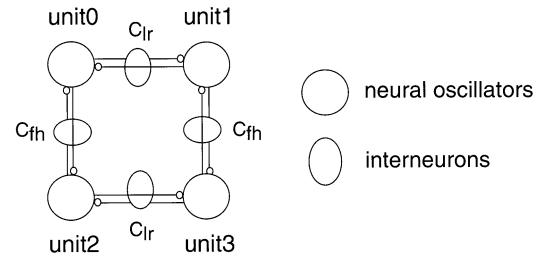

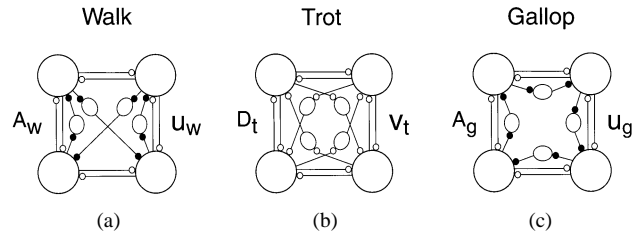
Fig. 5.   Basic configuration of the CPG network model.

Fig. 6.   Functional configuration corresponding to the typical gaits patterns in mammal. (a) Walk mode. (b) Trot mode. (c) Gallop mode.

By combining the networks that correspond to each of the gait modes, we construct the entire network. The network dynamics is given by the following equations:

$$\begin{aligned} \tau_u \dot{u}^{\{0,1,2,3\}} = &- u^{\{0,1,2,3\}} + A f_\mu(u^{\{0,1,2,3\}}) \\ &+ A_w f_\mu(u_w^{\{2,3,1,0\}}) + A_g f_\mu\left(u_g^{\{2,0,3,1\}}\right) \\ &- C_{lr} f_\mu(v^{\{1,0,3,2\}}) - C_{fh} f_\mu(v^{\{2,3,0,1\}}) \\ &- C f_\mu(v^{\{0,1,2,3\}}) + I_u^{\{0,1,2,3\}} \end{aligned} \quad (3)$$

$$\begin{aligned} \tau_v \dot{v}^{\{0,1,2,3\}} = &- v^{\{0,1,2,3\}} + B f_\mu(u^{\{0,1,2,3\}}) \\ &- D_t f_\mu(v_t^{\{3,2,1,0\}}) + I_v^{\{0,1,2,3\}} \end{aligned} \quad (4)$$

$$\begin{aligned} \tau_w \dot{u}_w^{\{0,1,2,3\}} = &- u_w^{\{0,1,2,3\}} + A_w f_\mu(u^{\{0,1,2,3\}}) \\ &+ I_{u_w}^{\{0,1,2,3\}} \end{aligned} \quad (5)$$

$$\begin{aligned} \tau_g \dot{u}_g^{\{0,1,2,3\}} = &- u_g^{\{0,1,2,3\}} + A_g f_\mu(u^{\{0,1,2,3\}}) \\ &+ I_{u_g}^{\{0,1,2,3\}} \end{aligned} \quad (6)$$

$$\begin{aligned} \tau_t \dot{v}_t^{\{0,1,2,3\}} = &- v_t^{\{0,1,2,3\}} - D_t f_\mu(v^{\{0,1,2,3\}}) \\ &+ I_{v_t}^{\{0,1,2,3\}} + I_{x_t}^{\{0,1,2,3\}} \end{aligned} \quad (7)$$
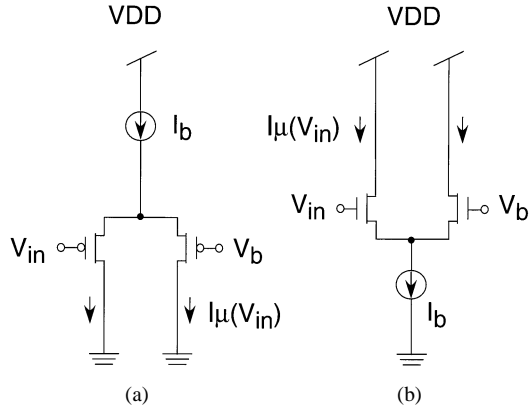
Fig. 7. Schematics of the differential pair circuits. (a) pMOS type. (b) nMOS type.

Fig. 8. Static responses of the differential pair (nMOS type).

where each index is an ordered set of four numbers, each of which correspond to a unit. u, u_w, and u_g represent activities of the excitatory neurons, v and v_t represent activities of the inhibitory neurons, $\tau_u, \tau_v, \tau_{u_w}, \tau_{u_g}$, and τ_{v_t} are the time constant of the neurons, A, A_w, A_g, B, C, C_{lr}, C_{fh}, and D_t are the interaction parameters. I_u, I_v, I_{u_w}, I_{u_g}, and I_{v_t} are the tonic bias inputs, and I_{x_t} is the external inputs.

Depending on the interaction parameters A through D_t, the tonic bias inputs I_u through I_{v_t} and the external inputs I_{x_t}, the dynamics of the network is determined. In particular, the bias inputs and the external inputs determine the equilibrium point of the network.

IV. ARCHITECTURE OF THE CPG CONTROLLER

In this section, we describe the architecture of the CPG controller for interlimb coordination in quadruped locomotion. First, the basic cell circuits that constitute a part of the CPG controller are given, next the architecture of the entire system is described.

A. Cell Circuits

We designed the cell circuits that constitute a part of the CPG controller. Each circuit consists of the basic analog CMOS circuits, such as the differential pair, the current mirror, and the translinear current multiplier/divider [23].

First, we describe the characteristics of the differential pair, which is one of the most fundamental components of the CPG controller. Fig. 7(a) and (b) each show two types of schematics of the differential pair. The differential pair can approximate the transfer function (2). When the MOS transistors, which comprise the differential pair, operate in their subthreshold region, the static response of the differential pair is given by the following equation [23]:

$$I_\mu(v_{in}) = I_b \frac{1 + \tanh(\mu(v_{in} - v_b))}{2} \qquad (8)$$

where v_{in} is the input voltage, v_b is the bias voltage, I_b is the bias current, $\mu = \kappa/2V_T$, V_T is the thermal voltage, and κ is the electrostatic coupling coefficient between the gate and
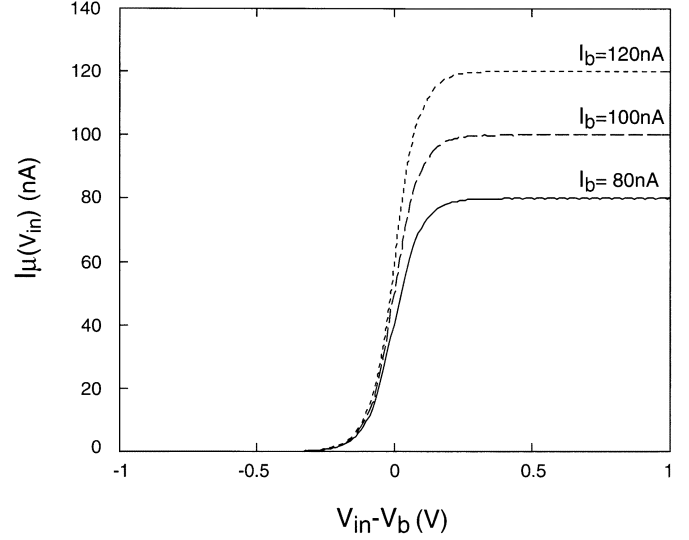
channel. Here, we show static responses of the nMOS type circuit in Fig. 8.

The excitatory cell circuit is shown in Fig. 9(a). It consists of the *RC* circuit, the differential pair circuit and the current source. The dynamics of the excitatory cell circuit is given by the following equation:

$$C_u \dot{u} = -\frac{u}{R_u} + I_u(t) \qquad (9)$$

where u expresses the voltage value, C_u is the capacitance value, R_u is the resistance value, and $I_u(t)$ is the external current that is independent of the voltage u. The excitatory cell circuit outputs positive current according to (8).

The inhibitory cell circuit is shown in Fig. 9(b). It also consists of the *RC* circuit, the differential pair circuit and the current source. The dynamics of the inhibitory cell circuit is given by the following equation:

$$C_v \dot{v} = -\frac{v}{R_v} + I_v(t) \qquad (10)$$

where v is the voltage value, c_v is the capacitance value, R_v is the resistance value, and $I_v(t)$ is external current that is independent of the voltage v. The inhibitory cell circuit outputs negative current according to (8).
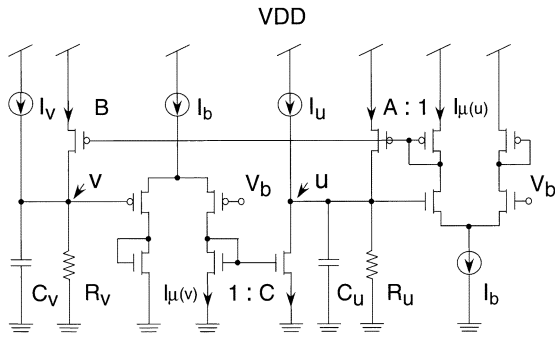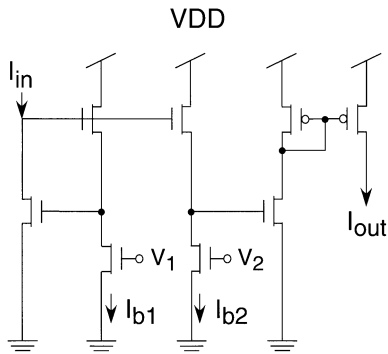

Fig. 9. (a) Schematic of the excitatory cell circuit. (b) Inhibitory cell circuit.

Fig. 10. Schematic of the neural oscillator cell circuit.

Fig. 11. Schematic of the translinear current multiplier/divider.

Fig. 12. Static responses of the translinear current multiplier/divider.

Fig. 13. Schematic of the complete neural oscillator cell circuit.

Fig. 10 shows the neural oscillator cell circuit whose dynamics is expressed by (1). We rewrite (1) as follows:

$$\begin{cases} C_u \dot{u} = -\dfrac{u}{R_u} + A \cdot I_\mu(u) - C \cdot I_\mu(v) + I_u(t) \\ C_v \dot{v} = -\dfrac{v}{R_v} + B \cdot I_\mu(u) + I_v(t) \end{cases} \tag{11}$$

where the parameters A–C are same in (3). $I(u)$ and $I(v)$ are the output currents of the differential pairs. The neural oscillator cell circuit consists of the excitatory cell circuit and the inhibitory cell circuit, and each variable corresponds to (7) and (8). The ratio of the interaction parameters is determined by the aspect ratio W/L (W: the gate width, L: the gate length) in the current mirrors. The circuit generates the periodic rhythmic pattern as a result of the interaction with the excitatory and inhibitory cell circuit. Depending on the parameters A through C and the external inputs $I_u(t)$ and $I_v(t)$, the circuit generates the periodic rhythmic pattern automatically.

If we want to regulate the frequency of the periodic rhythmic pattern, we should adjust the period of the limit cycle in the $u-v$ phase plane. Namely, we should properly adjust the balance of the interaction parameters, and the external inputs. To do this, it is necessary to adjust the balance between currents $A \cdot I_\mu(u)$ and $B \cdot I_\mu(u)$. By changing these currents, the equilibrium point in the dynamics has also been changed. Therefore, the bias currents should be regulated.

Hence, we combine the transliner current multiplier/divider with the neural oscillator cell circuit. Fig. 11 shows a schematic of the translinear current multiplier/divider. The circuit operates based on the transliner principle. Since all of the MOS transistors that comprise the circuit are operated in their subthreshold region, the dynamic range of the input and output currents are
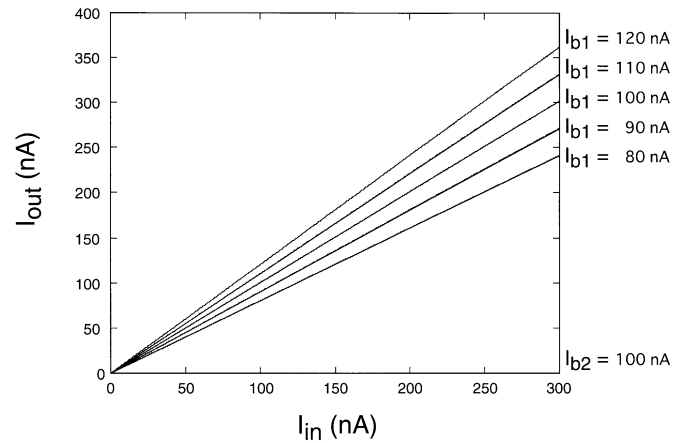
limited below an order of several hundreds nA. The static characteristic of the multiplier/divider is expressed as follows [23]:

$$I_{\text{out}} = \frac{I_{\text{in}} \cdot I_{b1}}{I_{b2}} = I_{\text{in}} \cdot \exp\left(\frac{\kappa(V_1 - V_2)}{V_T}\right) \tag{12}$$

where I_{in} is the input current, I_1 and I_2 are the bias current, and V_{b1} and V_{b2} are the bias voltage. Fig. 12 shows static characteristics of the transliner current multiplier/divider. In order to extend the dynamic range of the input/output currents, the gate width of all of the nMOS transistors comprising the circuit set at 12 μm.

Fig. 13 shows the complete neural oscillator circuit. Here, MD represents the translinear multiplier/divider. By adjusting the current $B \cdot I_\mu(u)$ using the transliner current multiplier/divider and the bias current I_v, we could regulate the frequency of the periodic rhythmic pattern generated by the neural oscillator cell circuit.

B. Network Architecture

We constructed the CPG controller from the cell circuits. Here, we use the excitatory cell circuit and the inhibitory cell circuit as the excitatory interneuron and the inhibitory interneuron, respectively. Let us rewrite (3)–(6) as follows:

$$\begin{aligned} C_u \dot{u}^{\{0,1,2,3\}} = &-\frac{u^{\{0,1,2,3\}}}{Ru} + A I_\mu(u^{\{0,1,2,3\}}) \\ &+ A_w I_\mu(u_w^{\{2,3,1,0\}}) + A_g I_\mu(u_g^{\{2,0,3,1\}}) \\ &- C_{lr} I_\mu(v^{\{1,0,3,2\}}) - C_{fh} I_\mu(v^{\{2,3,0,1\}}) \\ &- C I_\mu(v^{\{0,1,2,3\}}) + I_u^{\{0,1,2,3\}} \end{aligned} \tag{13}$$
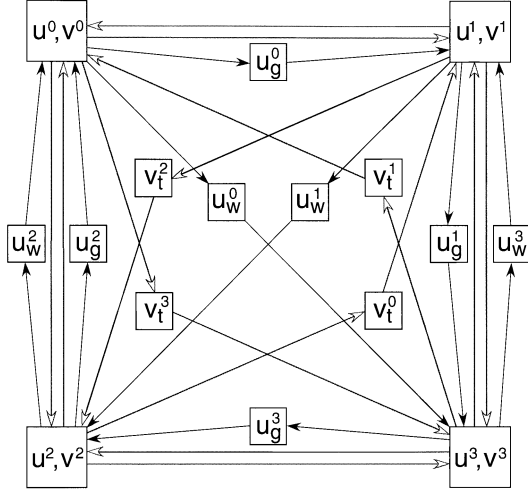
Fig. 14.   Entire network architecture of the CPG controller.

$$C_v \dot{v}^{\{0,1,2,3\}} = -\frac{v^{\{0,1,2,3\}}}{Rv} + Bf_\mu(v^{\{0,1,2,3\}})$$
$$- D_t I_\mu(v_t^{\{3,2,1,0\}}) + I_v^{\{0,1,2,3\}} \tag{14}$$

$$C_w \dot{u}_w^{\{0,1,2,3\}} = -\frac{u_w^{\{0,1,2,3\}}}{Ru_w} + A_w I_\mu(u^{\{0,1,2,3\}})$$
$$+ I_{uw}^{\{0,1,2,3\}} \tag{15}$$

$$C_g \dot{u}^{g\{0,1,2,3\}} = -\frac{u_g^{\{0,1,2,3\}}}{Ru_g} + A_g I_\mu(u^{\{0,1,2,3\}})$$
$$+ I_{ug}^{\{0,1,2,3\}}$$

$$C_t \dot{v}_t^{\{0,1,2,3\}} = -\frac{v_t^{\{0,1,2,3\}}}{Rv_t} - D_t I_\mu(v^{\{0,1,2,3\}})$$
$$+ I_{vt}^{\{0,1,2,3\}} + I_{xt}^{\{0,1,2,3\}} \tag{16}$$

where $I_\mu(\cdot)$ is the output current of the differential pair. The capacitance values C_u through C_{vt}, the resistance values R_u–R_{vt}, and the interaction parameters A–D_t correspond to those of (3)–(6). The ratio of the interaction parameters is determined by the aspect ratio W/L in the current mirrors. I_u^k, I_v^k, I_{uw}^k, I_{ug}^k and I_{vt}^k and $I_{xt}^k (k = 0, 1, 2, 3)$ are the DC bias currents, which control the equilibrium point of the CPG controller.

Fig. 14 shows a block diagram of the network architecture of the CPG controller, where the black and white arrow is excitatory and inhibitory interactions, respectively. Moreover, we use the voltage values v^k as outputs of the circuit, and each of them is transformed into torque driving actuator that control each of the limbs.

As a result of switching the operation of the interneurons that interact with the neural oscillator circuits, for instance, by using CMOS switch, the *functional reconfigurations* of the CPG controller are performed. Hence it follows that the transitions between different rhythmic patterns are achieved.

V. SIMULATION RESULTS

In this section, we confirm the operation of the proposed CPG controller through computer simulation. In the following simulation, we used the circuit simulator PSPICE and MOSIS AMIS

1.5-μm CMOS technology LEVEL 3 model parameters. As typical device parameters, $I_0 = O(10^{-16})$ A and $\kappa = 0.6$ are assumed. As common parameters, the gate length $L = 1.5$ μm, the capacitance values C_u, C_v, C_{ug}, C_{vt}, and C_{uw} were set at (100, 100, 100, 100, 300) nF, the resistance values R_u, R_v, R_{u_w}, R_{u_g}, and R_{v_t} were set at 1 MΩ, the interaction parameters A, B, C, C_{lr}, and C_{fh} were set as follows:

$$A = C = 4.0 \quad B = 3.0 \quad C_{lr} = C_{fh} = 1.0$$

where the gate width of minimum size of nMOS and pMOS transistors were set at (2.4, 4.8) μm. Furthermore, we set the bias currents of the differential pairs at 100 nA.

A. Production of Multiple Gait Patterns

First, we confirmed the generation of the periodic rhythmic patterns in the circuit. Three examples of the rhythmic patterns of voltage values v^k in the circuit are shown in Fig. 15(a)–(c). It is shown that each periodic rhythmic pattern corresponds to the gait patterns such as walk, trot, and gallop.

Fig. 15(a) corresponds to the walk mode. In the mode, we set the interaction parameters as follows:

$$A_w = 2.0 \quad A_g = D_t = 0.0.$$

The bias currents I_u, I_v, I_{uw}, I_{ug}, and I_{vt} were set at 0.95, 0.95, 0.85, 1.0, 1.0 μA, the bias currents I_{xt}^k were set at 0 A ($k = 0, 1, 2, 3$).

Fig. 15(b) corresponds to the trot mode. In the mode, we set the interaction parameters as follows:

$$D_t = 1.0 \quad A_w = A_g = 0.0.$$

The bias currents I_u, I_v, I_{uw}, I_{ug}, and I_{vt} were set at 1.1, 0.9, 1.0, 1.0, 1.05 μA, the bias currents I_{xt}^0 I_{xt}^1 I_{xt}^2 and I_{xt}^3 were set at 2, 0, 0, 2 nA.

Fig. 15(c) corresponds to the gallop mode. In the mode, we set the interaction parameters as follows:

$$A_g = 3.0 \quad A_w = D_t = 0.0.$$

The bias currents I_u, I_v, I_{uw}, I_{ug}, and I_{vt} were set at 1.0, 0.85, 1.0, 0.9, 1.0 μA, the bias currents I_{xt}^k were set at 0 A ($k = 0, 1, 2, 3$).

B. Gait Pattern Transitions

Second, we confirmed to occur the transition between the different rhythmic patterns in the circuit. In the following simulation, the interaction parameters and the bias currents were changed at 5.0 s. Fig. 16(a) and (b) shows two examples of transitions in the circuit. Fig. 16(a) and (b) corresponds to the transition from walk to trot and from trot to gallop, respectively. In each mode, it is shown that the circuit has the capability to change the rhythmic patterns promptly.

C. Regulation of Oscillatory Frequency

Third, we regulated the frequency of the periodic rhythmic pattern in the circuit. In order to regulate the frequency of the rhythmic pattern, it is necessary to adjust the balance between currents $A \cdot I_\mu(u^k)$ and $B \cdot I_\mu(u^k)$, and the bias currents I_v^k. By
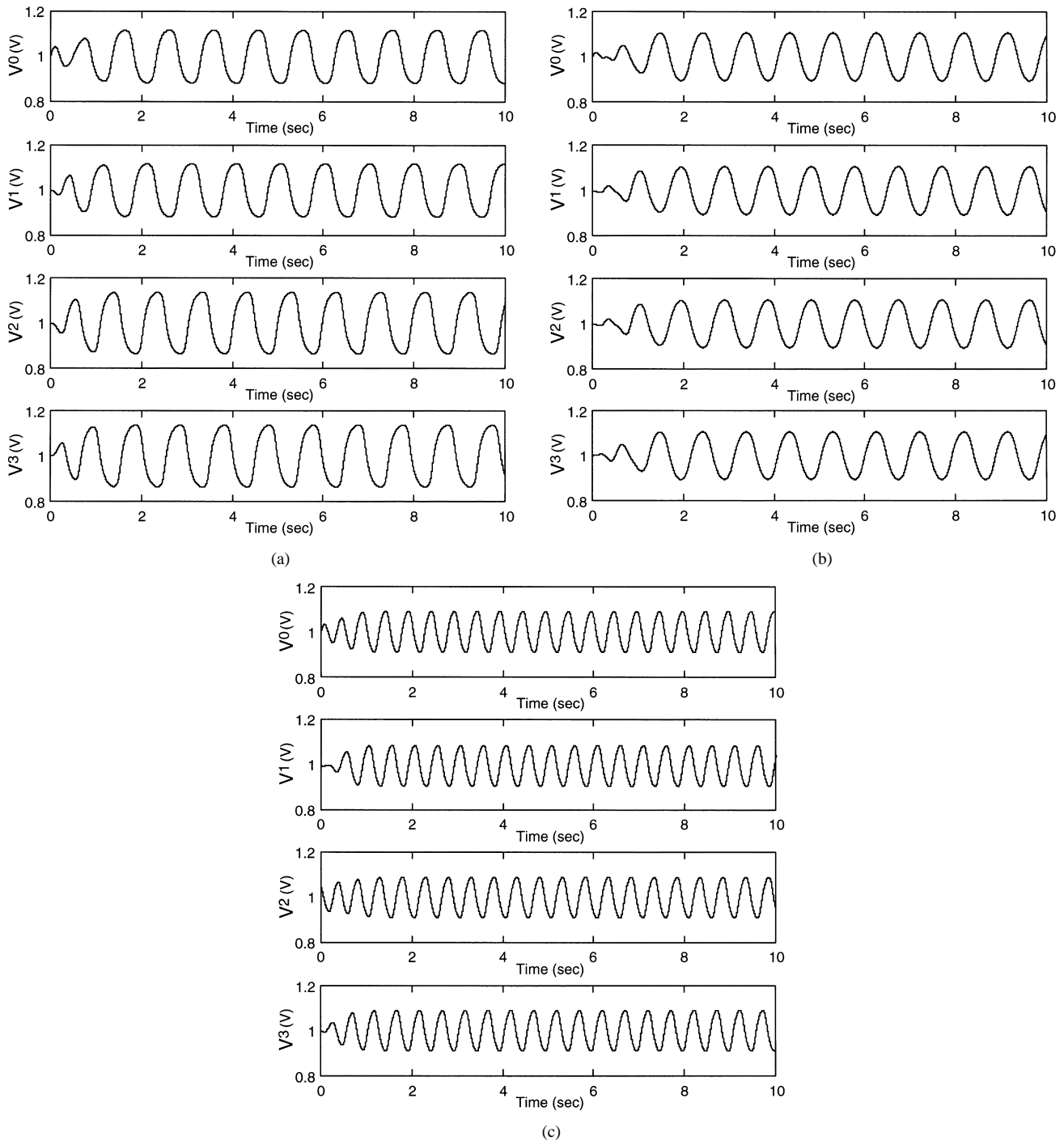
Fig. 15. Rhythmic patterns corresponding to each of the gait patterns. (a) Walk mode. (b) Trot mode. (c) Gallop mode.

regulating the currents $B \cdot I_\mu(u^k)$ and I_v^k, the frequency of the rhythmic pattern could be regulated.

Fig. 17 shows the regulation of the frequency in trot mode. At 0 to 10.0 s, we set the bias currents in the translinear current multiplier/divider (I_{b1}, I_{b2}) at (120 nA, 120 nA), the bias currents I_v^k at 900 nA ($k = 0, 1, 2, 3$). Then, the frequency of the periodic rhythmic pattern is about 1.0 Hz.

Furthermore, at 10.0–20.0 s, we change the bias current I_{b1} toward 200 nA and the bias currents I_v^k toward 800 nA continuously. Then, the frequency of the periodic rhythmic pattern is changed from about 1.0 to 1.4 Hz.

D. Influence of Disturbance

In Fig. 18, we give two weak disturbances to the circuit in the trot mode. The external current 250 nA and -250 nA is given to node u of unit 0 in the circuit at 5.1 to 5.2 s and at 8.2 to 8.3 s, respectively.

It is shown that the circuit has the stability against the disturbance. It is assumed that the stability is provided by the characteristics of the rhythmic patterns as an attractor of the CPG network. If disturbance is considered to be an input from a sensory neuron, the phase of the periodic pattern would be regulated by sensory feedback.
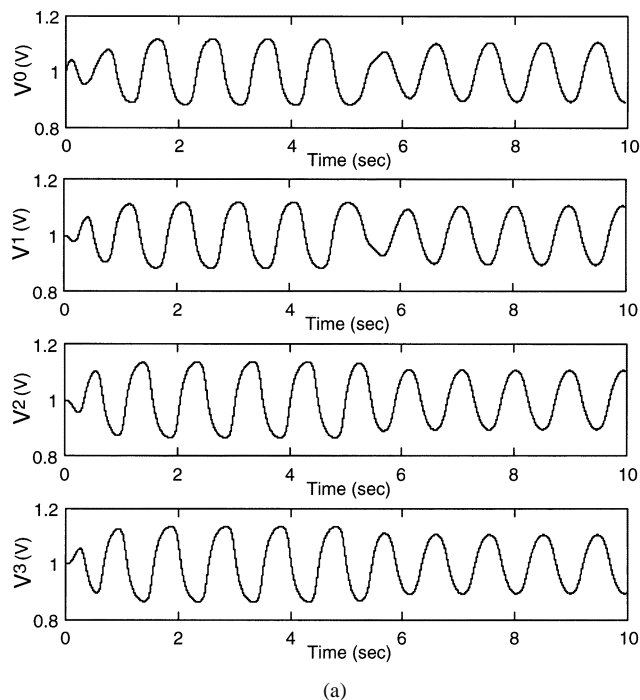
(a)
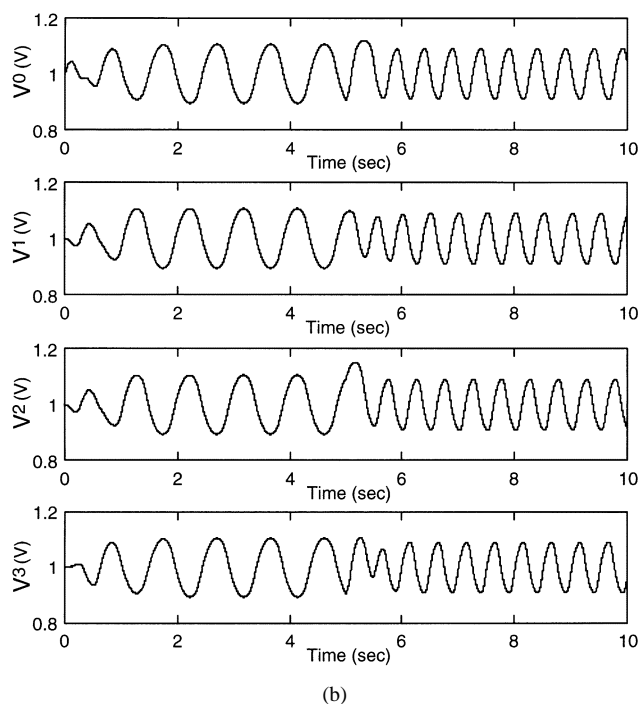
(b)

Fig. 16. Transitions between the differential periodic rhythmic patterns. (a) From walk to trot mode. (b) From trot to gallop mode.

Fig. 17. Regulation of the frequency of the periodic rhythmic patterns.
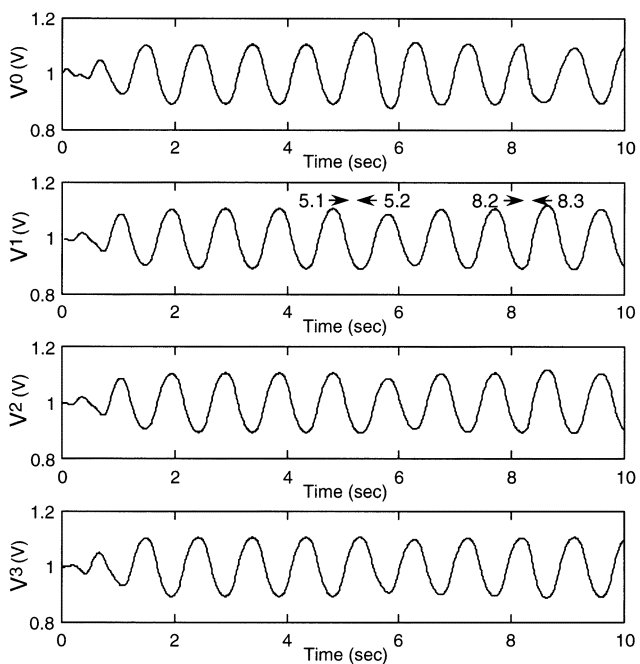
Fig. 18. Influence of disturbance on the periodic rhythmic patterns.

Through several computer simulations, we confirmed the desire operations of the proposed circuit. First, we confirmed that the circuit is capable to produce various rhythmic periodic patterns corresponding to the gait patterns. Second, we confirmed to occur the transitions from one pattern to another. Third, we also observed that it is possible to regulate the frequency of the periodic rhythmic patterns in the trot mode. Furthermore, we confirmed that the circuit has the stability against weak disturbance.

In the present simulations, we considered only three configurations corresponding to the walk mode, the trot mode and
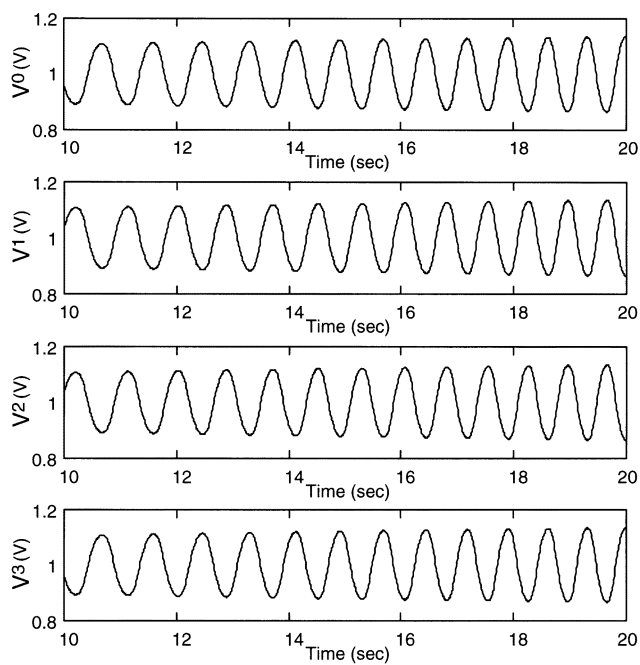
the gallop mode. However, more interneurons and connections between the oscillators, then more rhythmic patterns would be generated. Our CPG controller is designed not to give the real motion of each limb but only the timing of motion, since it is considered that the motion pattern of each limb is controlled by the lower nervous system and CPG to control interlimb coordination gives only the timing and the period of the motion of each limb in animal locomotion [22]. As the results, it is shown that the proposed circuit is sufficient as the CPG controller for interlimb coordination in quadruped locomotion.

VI. FURTHER CONSIDERATIONS

In this section, we examine practical problems in circuit implementation, which should be attendant to further studies.

When we construct our CPG controller, device fluctuations should affect accuracy of the operation of the circuit. In particular, the subthreshold operation of the circuit is affected strongly by the device fluctuations. Hence, we consider how each device parameter would affect the operation of operation.

First, we consider the device fluctuations in the MOS transistors. In the differential pair, the circuit operation depends on good matching between the MOS transistors that comprise the circuit. In the subthreshold region, the pre-exponential constant I_0 affects strongly accuracy of the circuit operation. In order to obtain high relative accuracy, we should place the pair of the MOS transistors comprising the differential pair closely. In the current mirror, furthermore, the matching of the aspect ratio is necessary since the ratio of the current mirror determines the dynamics of the CPG.

Second, we consider the fluctuation of resistors in the CPG controller. Since their fluctuations affect the equilibrium point in the CPG, their relative accuracies are important. Similarly, it is desirable to set the bias currents in the circuit, which determine the equilibrium point in the CPG, as accurately as possible.

In the present simulation, we use the large capacitors and resistors. This mean that when we try to built a chip with such capacitors and resistors, they would occupy a large area of the chip. In order to overcome such problems, we use external capacitors and resistors. By using such strategy, small area of chips and low-cost production can be realized.

VII. SUMMARY

In this paper, we proposed an analog CMOS controller for interlimb coordination in quadruped locomotion. The proposed controller is based on the biological neural network, called CPG. In recent years, many researches have proposed CPG controllers for walking robots. While most of these have used digital processors that have several problems such as high power consumption, we designed the CPG controller as analog circuit.

In previous works, several analog CPG controllers have already been developed [11]–[13]. The present work differs from them in several respects. First, the CPG controller is based on the Amari–Hopfield model, which can be implemented easily with the fundamental analog circuits, such as the differential pair and the current mirror. Second, the CPG controller has the capability of generating several rhythmic patterns and changing their patterns promptly. These properties are sufficient for the CPG controller to coordinate interlimb motion in quadruped walking robots.

Furthermore, the CMOS transistors in the CPG controller operate in their subthreshold region and under low supply voltage, so it can reduce power consumption. Since a number of the transistors comprising the controller are less than a thousand, it is expected that low-cost production and miniaturization of chips can be realized.

Following the present research, we are going to develop autonomous adaptive controller for micro locomotor robots.

REFERENCES

[1] F. Delcomyn, "Neural basis of rhythmic behavior in animals," *Science*, vol. 210, pp. 492–498, 1980.
[2] M. Arbib, Ed., *The Handbook of Brain Theory and Neural Networks*, 2nd ed. Cambridge, MA: MIT Press, 2002.
[3] F. Delcomyn, *Foundations of Neurobiology*. New York: Freeman, 1997.
[4] A. I. Dagg, "Gait in mammals," *Mammal Rev.*, vol. 3, pp. 135–154, 1973.
[5] J. Nishii, "Legged animals select the optimal locomotor pattern based on energetic cost," *Biol. Cybern.*, vol. 83, pp. 435–442, 2000.
[6] S. L. Hooper, "Neural circuit: Functional reconfiguration," in *Encyclopedia of Life Sciences*. New York: Macmillan, 2000.
[7] H. Kimura, Y. Fukuoka, and K. Konaga, "Adaptive dynamic walking of a quadruped robot by using neural system model," *Advanced Robot.*, vol. 15, pp. 859–876, 2001.
[8] A. Billard and A. J. Ijspeert, "Biologically inspired neural controllers for motor control in a quadruped robot," presented at the *Int. Joint Conf. Neural Networks*, July 2000.
[9] J. Shan and F. Nagashima, "Neural locomotion controller design and implementation for humanoid robot hoap-1," presented at the 20th Annu. Conf. Robot. Soc. Japan, Osaka, Japan, 2002.
[10] A. Fujii, N. Saito, K. Nakahira, A. Ishiguro, and P. Eggenberger, "Generation of an adaptive controller CPG for a quadruped robot with neuromodulation mechanism," presented at the IEEE Int. Conf. Intell. Robots Syst., 2002.
[11] S. Still and M. W. Tilden, "Controller for a four legged walking machine," in *Neuromorphic Systems: Engineering Silicon from Neurobiology*, S. Smith and A. Hamilton, Eds, Singapore: World Scientific, 1998, pp. 138–148.
[12] G. Patel, J. Holleman, and S. Deweerth, "Analog VLSI model of intersegmental coordination with nearest neighbor coupling," *Adv. Neural Inform. Processing Syst.*, vol. 10, pp. 710–725, 1998.
[13] M. A. Lewis, M. J. Hartmann, R. Etienne-Cummings, and A. H. Cohen, "Control of a robot leg with an adaptive a VLSI CPG chip," *Neurocomput.*, vol. 38–40, pp. 1409–1421, 2001.
[14] S. Amari, "Characteristic of the random nets of analog neuron-like elements," *IEEE Trans. Syst., Man, Cybern.*, vol. SMC-2, pp. 643–657, 1972.
[15] H. R. Wilson and J. D. Cowan, "Excitatory and inhibitory interactions in localized populations of model neurons," *Biophys. J.*, vol. 12, pp. 1–24, 1972.
[16] G. Brown, "On the nature of the fundamental activity of the nervous centers; together with an analysis of the conditioning of the rhythmic activity in progression, and a theory of the evolution of function in the nervous system," *J. Physiol.*, vol. 48, pp. 18–46, 1914.
[17] K. Matsuoka, "Mechanism of frequency and pattern control in the neural rhythm generators," *Biol. Cybern.*, vol. 56, pp. 345–353, 1987.
[18] G. Taga, Y. Yamaguchi, and H. Shimizu, "Self-organized control of bipedal locomotion by neural oscillators in unpredictable environment," *Biol. Cybern.*, vol. 65, pp. 147–159, 1991.
[19] H. Nagashino, Y. Nomura, and Y. Kinouchi, "Generation and transitions of phase-locked oscillations in coupled neural oscillators," presented at the 40th SICE Annu. Conf., Nagoya, Japan, 2001.
[20] S. Ito, H. Yuasa, Z. W. Luo, M. Ito, and D. Yanagihara, "A mathematical model of adaptive behavior in quadruped locomotion," *Biol. Cybern.*, vol. 78, pp. 337–347, 1998.
[21] R. D. Beer, H. J. Chiel, and J. C. Gallagher, "Evolution and analysis of model CPG's for walking ii. General principles and individual variability," *J. Comput. Neurosci.*, vol. 7, pp. 119–147, 1999.
[22] H. Yuasa and M. Ito, "Coordination of many oscillators and generation of locomortory patterns," *Biol. Cybern.*, vol. 63, pp. 177–184, 1990.
[23] M. Isamail and T. Fiez, *ANALOG VLSI, Signal and Information Processing*. New York: McGraw-Hill, 1993.
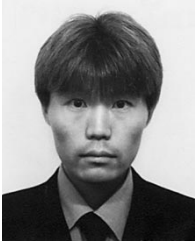
Kazuki Nakada (S'02) received the B.S. degree in mathematics in 1999 and the M.E. degree from the Department of Systems and Information Engineering, Hokkaido University, in 2002, both from Hokkaido University, Sapporo, Japan. He is currently working toward the Dr. Eng. degree in the Department of Electrical Engineering, Hokkaido University.

His current research interests include biologically inspired robotics and neuromorphic analog/digital systems.

Yoshihito Amemiya (M'97) received the B.E., M.E., and Dr. Eng. degrees from the Tokyo Institute of Technology, Tokyo, Japan, in 1970, 1972, and 1975, respectively.

From 1975 to 1993, he was with NTT LSI Laboratory, Atsugi, Japan. Since 1993, he has been a Professor in the Department of Electrical Engineering, Hokkaido University, Sapporo, Japan. His research interests are in electronic circuits, large-scale integration (LSI) circuits, functional devices based on nonlinear analog computation, logic systems using single-electron circuits, and information-processing devices using quantum-effect nanostructures.

Tetsuya Asai (M'01) received the B.E. and M.E. degrees in electrical engineering from Tokai University, Kanagawa, Japan, in 1993 and 1996, respectively, and the Dr. Eng. degree in electrical and electronic Engineering from the Toyohashi University of Technology, Aichi, Japan, in 1999.

He is now an Associate Professor in the Department of Electrical Engineering, Hokkaido University, Sapporo, Japan. His current research interests include sensory information processing in neural networks as well as design and applications of neuromorphic VLSIs and the reaction-diffusion chip.